HHS Public Access

Author manuscript

Nat Neurosci. Author manuscript; available in PMC 2019 December 24.

Published in final edited form as:

Nat Neurosci. 2019 August ; 22(8): 1269–1275. doi:10.1038/s41593-019-0424-1.

Chondroitinase Improves Anatomical and Functional Outcomes After Primate Spinal Cord Injury

Ephron S. Rosenzweig[1], **Ernesto A. Salegio**[2], **Justine J. Liang**[1], **Janet L. Weber**[1], **Chase A. Weinholtz**[1], **John H. Brock**[1,3], **Rod Moseanko**[2], **Stephanie Hawbecker**[2], **Roger Pender**[2], **Christina L. Cruzen**[2], **Jennifer F. Iaci**[4], **Anthony O. Caggiano**[4], **Andrew R. Blight**[4], **Barbara Haenzi**[5], **J. Russell Huie**[6], **Leif A. Havton**[7], **Yvette S. Nout-Lomas**[8], **James W. Fawcett**[5], **Adam R. Ferguson**[6], **Michael S. Beattie**[6], **Jacqueline C. Bresnahan**[6], **Mark H. Tuszynski**[1,3]

[1]Dept. of Neurosciences, University of California - San Diego, La Jolla, CA [2]California National Primate Research Center, University of California, Davis, CA [3]Veterans Administration Medical Center, La Jolla, CA [4]Acorda Therapeutics, Ardsley, NY [5]Cambridge University, Cambridge, England [6]Dept. of Neurosurgery, University of California, San Francisco, CA [7]Depts. Neurology and Neurobiology, University of California, Los Angeles, CA [8]College of Veterinary Medicine and Biomedical Sciences, Colorado State University, Fort Collins, CO

Abstract

Inhibitory extracellular matrices form around mature neurons as perineuronal nets containing chondroitin sulfate proteoglycans (CSPGs) that limit axonal sprouting after CNS injury. The enzyme chondroitinase (Chase) degrades the inhibitory CSPGs and improves axonal sprouting and functional recovery after spinal cord injury (SCI) in rodents. We evaluated the effects of Chase in Rhesus monkeys that had undergone C7 spinal cord hemisection. Four weeks after hemisection, multiple intraparenchymal Chase injections targeted spinal cord circuits controlling hand function below the lesion. Hand function improved significantly in Chase-treated monkeys relative to vehicle-injected controls. Moreover, Chase significantly increased corticospinal axon growth and the number of synapses formed by corticospinal terminals in gray matter caudal to the lesion. No detrimental effects were detected. This approach appears to merit clinical translation in SCI.

Correspondence to: Mark H. Tuszynski, Dept. Neurosciences, 0626, University of California, San Diego, La Jolla, CA 92093, 858-534-8857, 858-534-5220 (fax), mtuszynski@ucsd.edu (email).

AUTHOR CONTRIBUTIONS:

ESR, EAS, JHB, JFI, AOC, ARB, JRH, LAH, JFI, AOC, ARB, YSN-L, ARF, MSB, JCB, and MHT designed experiments.
ESR, EAS, RM, SH, RP, CLC, JFI, AOC, ARB, YSN-L, JCB, and MHT carried out experiments.
ESR, EAS, JJL, JLW, CAW, JHB, BH, JRH, JWF, ARF, MSB, JCB, and MHT analyzed data.
ESR and MHT wrote the manuscript.
ESR, EAS, JJL, JLW, CAW, JHB, RM, SH, RP, CLC, JFI, AOC, ARB, BH, JRH, LAH, YSN-L, JWF, ARF, MSB, JCB, and MHT edited the manuscript.

COMPETING INTERESTS:

JFI, AOC and ARB are employees of Acorda Therapeutics, Inc., and JWF and MHT were members of the Acorda scientific advisory board at the time that these studies were performed. All other authors declare no competing interests.

A number of mechanisms limit the regenerative capacity of the injured adult mammalian central nervous system (CNS), including insufficient trophic support and the presence of inhibitors to axon growth associated with both myelin and the extracellular matrix (ECM) [1,2]. Among the ECM molecules that inhibit axon growth, a major contribution is made by chondroitin sulphate proteoglycans (CSPGs) [3,4]. The predominant CSPG molecules that are present in the CNS include NG2, neurocan and aggrecan [5–7], which consist of a core protein with long, sulfated glycosaminoglycan (GAG) side chains. The side chains are the primary determinants of axon inhibition [8]. As the period of robust developmental plasticity of the nervous system closes, CSPGs form around neurons and synapses in “peri-neuronal nets” that are postulated to influence the function of the CNS by controlling plasticity and sprouting [9]. In addition, CSPGs are newly synthesized at sites of CNS injury and directly block axon growth [5–8,10–12].

The natural bacterial enzyme chondroitinase ABC (Chase) can degrade the inhibitory carbohydrate side chains on CSPGs [3,4,13,14]. Indeed, Chase administration to rats after spinal cord injury (SCI) enhances growth of both corticospinal and sensory axons, and improves functional outcomes [3,4,14–16]. These growth-promoting effects of Chase result from removal of perineuronal nets, which increases sprouting from spared axons below the injury site and formation of new synaptic connections [17,18]. Alternatively, when a cellular or peripheral nerve bridge is placed into a spinal cord lesion site, Chase can promote axonal regeneration of cut axons into the bridge [10,19]. Beneficial effects of Chase administration have been reported in rodent models of SCI [3,4,10,14–16,18,20], nigrostriatal injury [13] and stroke [21–23] and cats with SCI [24,25].

Novel therapies to promote CNS sprouting and regeneration are needed to improve outcomes after human neurotrauma and stroke. Given the replication of Chase efficacy across multiple experimental models by independent laboratories, together with the identification of compelling candidate mechanisms underlying its beneficial effects, we advanced Chase therapy to a non-human primate model of SCI as a potential prelude to human clinical trials. Primates, both human and non-human, exhibit potentially important differences from rodents in size, anatomy, systems function and immunology that make predictions of human safety and benefit based solely on rodent studies uncertain, a concern highlighted by numerous failed trials in stroke, spinal cord injury and other disorders [26–29]. We first employed a porcine model to test methods for Chase administration in the large animal spinal cord, and found that intrathecal infusions failed to degrade CSPGs in spinal cord gray matter. We accordingly moved to intraparenchymal spinal cord injections of Chase; these effectively degraded CSPGs in our rhesus monkey model of C7 spinal cord lateral hemisection [30]. This experiment hypothesized that degradation of perineuronal nets surrounding neurons in spinal cord gray matter below the lesion would enhance sprouting of spared host axonal systems, including the corticospinal tract (CST), the most important motor system for voluntary movement in primates [31,32]. Previously, we reported spontaneous sprouting of spared corticospinal axons in monkeys after C7 lesions [30], supporting their potential relevance as a target for enhanced growth after human SCI, where the majority of lesions spare a superficial rim of white matter including corticospinal axons [33,34]. Thus, using intraparenchymal injections, we tested Chase administration in rhesus monkeys with hemisections, comparing experimental and control lesion subjects.

RESULTS:

Route of Chase Administration: Successful Delivery by Intraparenchymal but Not Intrathecal Infusion

In a preliminary study, we determined whether intrathecal injections of Chase, a frequent and effective route of administration in rat studies, would effectively diffuse into the spinal cord of a larger animal. We used pigs for this study because their spinal cords measure roughly 8–11 mm in diameter (compared to rat 3.5 mm width and human 12.5 mm width). Seven adult American Yorkshire-Landrace-Duroc pigs received intermittent (every other day for two weeks) intrathecal injections of 2 ml of saline (N=1), 5 Units Chase enzyme/ml (5 U/ml, 10 U/dose; N=3 animals; For Chase, 1 U is the amount that catalyzes the conversion of 1 micro-mole of chondroitin sulfate A or C per minute at 37°C and pH 8.0), or 25 Units Chase enzyme/ml (50 U/dose; N=3 animals) (Chase provided by Acorda Therapeutics). Injections were made at 0.2 ml/min via an indwelling catheter into the intrathecal space between vertebrae T11–13. Pigs were sacrificed two days after the last dose of intrathecal Chase. With this infusion method, 2B6 immunohistochemistry revealed degradation of GAG side chains in both low-dose and high-dose groups in a 1mm rim of the *superficial* circumferential thoracic spinal cord white matter (Suppl. Fig. 1A,B). However, peri-neuronal nets in spinal cord gray matter were *not* attenuated, as revealed by *wisteria floribunda agglutinin* (WFA) lectin-histochemistry (Suppl. Fig. 1C,D). Because a prime target of Chase therapy is removal of peri-neuronal inhibitory CSPGs in gray matter to enhance plasticity and new synapse formation, we concluded that intrathecal infusions of the current formulation of Chase in the larger spinal cord were *not* an effective delivery method to enable hypothesis testing in the primate model, and (in the absence of a more parenchymal-penetrant formulation or method for Chase administration) we moved to intraparenchymal injections in monkeys.

In a preliminary study to test the delivery efficacy of *intraparenchymal* Chase administration in monkeys, two adult rhesus male monkeys underwent C7 spinal cord hemisection lesions [30,35] followed four weeks later by intraparenchymal injections of Chase. Four weeks post lesion is a time point at which spontaneous plasticity in the primate is occurring (see below). Monkeys received injections of 20 U/ml Chase starting at spinal cord level C7 (1 mm caudal to the lesion). 5 μl of Chase were injected at each of 10 sites (spaced 1.5 mm apart in the rostrocaudal axis) on the right side of the spinal cord from C7–T1. Chase was infused at two dorsoventral depths per injection site, the first targeting the intermediate gray (2.5 mm depth) and the second targeting the ventral gray (3.5 mm depth). 2.5 μl were injected at each depth (infusion rate 0.5 μl/ml) for a total volume of 5 μl per site (Fig. 1). As noted above, the primary objective of this injection design is to degrade peri-neuronal CSPG “nets” that surround adult neurons in host gray matter below the lesion site, to enhance sprouting from spared host axons [10,15,18] that occurs spontaneously after SCI [30,36–41]. We did not attempt to promote regeneration into the lesion site by grafting cellular or peripheral nerve bridges into the lesion cavity [10,14,19]. Subjects were transcardially perfused 2 weeks later to assess CSPG degradation by WFA histochemistry. CSPGs were completely degraded in the spinal cord gray matter over a distance of at least 2mm from each injection site without evident damage to the spinal cord or neuronal loss (Fig. 2, Suppl. Figs. 2–4). We therefore

used the same injection design to deliver Chase to the subjects in the therapeutic efficacy study (see below). CSPGs were also degraded at the caudal aspect of the C7 spinal cord lesion site (Suppl. Fig. 5).

Chase Therapeutic Efficacy Study in Non-Human Primates

A total of 12 adult male rhesus monkeys underwent C7 right-sided complete spinal cord hemisection lesions, which result in persistent deficits in right hand dexterity but retention of bowel/bladder function and locomotion [30,35,39,42]. While this lesion results in extensive impairment in right hand function immediately after the lesion, there is consistent, predictable, but incomplete recovery from 4–8 weeks post-lesion, with little further improvement thereafter [30,35,39,42]. Hypothesizing that the period of recovery from 4–8 weeks is mediated by spontaneous anatomical plasticity, we injected Chase four weeks post-injury to target enhancement of endogenous plasticity. This delay was also chosen because it is a clinically *practical* time to intervene after SCI, when most medical complications in humans have stabilized and patients are better candidates to undergo surgical intervention [43]. Moreover, the extent of functional deficit and probability of further spontaneous clinical recovery can be assessed more reliably in humans four weeks post-injury than within days of injury, considerations that are helpful in designing a clinical trial.

The primate C7 lesion model was designed to assess potential therapies for improving hand function, since neural circuitry for hand control is located in the C7–T1 spinal levels ranging from 1 mm to 15 mm below the lesion. These segments received intraparenchymal injections of Chase (20 U/ml) four weeks after lesions were placed, as indicated above (Fig. 1). Four days later, monkeys underwent daily half-hour exposure to a large testing enclosure enriched with numerous objects, perches, and food rewards to encourage use of both forelimbs and hindlimbs [42,44]. Monkeys engage in naturalistic and reward-driven behaviors in this environment [42,44]. Once per week, several functions in the enclosure were evaluated and scored on an ordinal scale by an observer blinded to treatment condition [42,44]. Some of these functional measures are sensitive to forelimb performance (Suppl. Fig. 6) and others to hindlimb performance; yet other scores represent composites of overall function (Fig. 3). Separately, monkeys underwent daily exposure to a cage-based Brinkman board task with graded levels of difficulty, requiring retrieval of small food items from baited wells using only the affected right arm (Fig. 3). There were five levels of difficulty on this task, and monkeys were scored weekly on each level. A total of 12 monkeys underwent C7 lesions: 6 received injections of Chase and 6 were lesioned controls. Of the lesioned controls, 4 monkeys received injections of 5 μl/site of saline; 1 underwent needle entry only into each site; and 1 monkey underwent sham surgery to expose the spinal cord, without needle entry or saline injection. No differences were noted between these control subjects on any measured parameter, and their data were combined in the subsequent analyses. Three months after Chase administration or control injections, subjects underwent anterograde tracing of the corticospinal projection with biotinylated dextran amine in the left hemisphere and dextran-conjugated Alexa-Fluor 488 in the right hemisphere [45], and were transcardially perfused 6 weeks later (5.5 months after the initial lesion). One control subject was excluded post-hoc from behavioral analyses on the basis of over-lesion that extended onto the right side of the spinal cord (see Suppl. Fig. 7). An additional control subject did

not undergo corticospinal tracing due to weight drop below the minimum level required to allow surgery.

Chase Administration Improves Functional Outcomes

We performed a non-linear principal components analysis (NL-PCA; see Methods) on the ensemble of all behavioral outcome data from the exercise enclosure and the Brinkman board (Fig. 3; N=6 Chase subjects and N=5 Control subjects). Behavioral measures loaded highly on the first principal component (PC1), which accounted for 68% of the variance in recovery (Suppl. Fig. 8). The resulting weights for each measure were then extracted to create PC scores for each animal at each timepoint. The PC1 scores were then used to test for group differences in performance over time. Overall, PC1 showed a significant difference between lesioned controls and Chase-treated animals over time, favoring the Chase-treated group (condition × time, $F_{(9, 23.87)} = 5.15$, P = 0.001, AIC = 94.21, linear mixed model; Fig. 3A). Lesioned control animals in this study followed a previously reported pattern (noted above) [30,42] of marked impairment in function post-lesion, relative to their pre-lesion baseline, for the first four weeks after C7 hemisection (Fig. 3). This was followed by spontaneous recovery of function (reflected by the PC1 scores) over weeks 5–8 (Fig. 3A). The function of lesioned controls did not significantly improve further, from weeks 5–8 through weeks 17–20 (main effect of time, $F_{(3, 12)} = 1.87$, P = 0.189, $\eta_p^2 = 0.319$, repeated measures ANOVA; Fig. 3A; Suppl. Video 1). Animals treated with Chase also exhibited marked impairment in hand function over the first 4 weeks post-lesion, followed by early spontaneous improvement by weeks 5–8. However, in contrast to the lesioned control group, animals in the Chase treatment group exhibited *continued* improvement from weeks 5–8 to weeks 17–20 (main effect of time, $F_{(3, 15)} = 7.53$, P = 0.003, $\eta_p^2 = 0.601$, repeated measures ANOVA; Fig. 3A; Suppl. Video 2). Analysis of performance on individual tasks showed divergence that favored Chase-treated subjects on measures sensitive to right hand use (Fig. 3D–I) but not locomotion (Fig. 3J). This observation is consistent with the delivery of Chase to spinal cord segments influencing hand function. In terms of absolute performance levels, monkeys that received Chase exhibited an overall final food object retrieval success rate of 47 ± 12% across all difficulties of the Brinkman board in the final testing period, compared to nearly 100% pre-injury performance and an inability to retrieve objects in the first four weeks after injury. In comparison, lesioned control monkeys recovered to 31 ± 14% final food object retrieval on the Brinkman board, compared to 5 ± 3% performance in the first four weeks after injury. This is a 51% difference between groups in the extent of recovery, favoring Chase. The difference in absolute performance between groups is significant (P = 0.014, linear mixed model, condition × time, $F_{(37, 12.48)} = 3.26$, AIC = 1461.5).

PCA also generated a second and third principal component that accounted for 10.5 % and 5.1% variance respectively (Suppl. Fig. 8). However, loading patterns for these components did not indicate clearly definable eigenmodules, and scores on these components were therefore not tested.

Chase Administration Improves Anatomical Outcomes

We hypothesized that, by degrading peri-neuronal nets in the gray matter surrounding neurons and synapses caudal to the C7 lesion site, Chase administration would increase

axonal sprouting and synaptogenesis from spared axonal systems. Previously we reported that, in rhesus monkeys, spared components of the corticospinal system that decussate across the spinal cord midline undergo spontaneous axonal sprouting after C7 hemisection lesions [30,39]. In Chase-treated subjects, we found greater total length (compared to control subjects) of corticospinal axons in gray matter caudal to the injury at C8, indicative of sprouting of spared corticospinal axons that decussate across the spinal cord midline [30,39] (N=6 Chase subjects and N=5 Control subjects; $F_{(1, 30.02)} = 4.81$, P = 0.036, AIC = 693.89, linear mixed model; Fig. 4C). The same Chase-associated increase in axon density (compared to control subjects) was observed in CST axons originating in the right motor cortex ($F_{(1, 43.13)} = 13.15$, P = 0.001, AIC = 1239.11, linear mixed model; Suppl. Fig. 9). All measures were made in a blinded fashion, and analysis of corticospinal axons arising from the left hemisphere was done in one laboratory (MHT), while analysis of axons arising from the right hemisphere was done independently in a second laboratory (JWF).

In addition, Chase treatment was associated with a significant increase, compared to lesioned controls, in the number of corticospinal synapses in gray matter caudal to the injury (N=6 Chase subjects and N=5 Control subjects; $F_{(1, 38.12)} = 12.06$, P = 0.001, AIC = 119.18, linear mixed model; Fig. 4). CST synaptic connectivity was assessed by quantifying the number of CST terminal boutons that co-localized with synaptophysin immunoreactivity, divided by the sampled volume of gray matter (Fig. 4E).

We also assessed whether serotonergic axons respond to chondroitinase treatment. In a previous study of lesioned animals lacking experimental treatment, serotonergic axons, in contrast to corticospinal axons, did not exhibit detectable sprouting after C7 hemisection lesions [30]. In the present study, we observed no difference between Chase and control subjects in total serotonergic axon length in motor neuron pools caudal to SCI (N=6 Chase subjects and N=5 Control subjects; Wald $\chi^2 = 0.009$, QIC = 4.86, P=0.924, generalized estimating equation; Suppl. Fig. 10). All anatomical measures were made by observers blinded to treatment group.

Safety

Anatomical analysis of injection sites with Nissl stain revealed no detectable toxicity after intraparenchymal spinal cord injections (Suppl. Fig. 2). We also quantified motor neurons in a series of sections straddling an injection site in each monkey, and found no neuron loss in Chase-injected vs. lesion control monkeys (Suppl. Fig. 3). In addition, we quantified IBA-1 labeling in gray matter adjacent to injection sites to assess microglial responses, and found no difference between Chase-injected, saline-injected, and lesion control groups (ANOVA, $F_{(2, 3.78)} = 0.11$, P=0.89; Suppl. Fig. 4). Moreover, cellular-mediated inflammation in gray matter, assessed by labeling for CD8, CD3, and CD45, was extremely mild 2 weeks after Chase injection (Suppl. Fig. 3; CD8 labeling shown). Labeling for CD8, CD3, and CD45 was no longer detectable 4.5 months after injections of either Chase or saline (Suppl. Fig. 3). Systemically, Chase-treated and lesioned control monkeys exhibited no notable differences in weight, activity or post-lesion complications. Although formal pain tests were not employed, monkeys exhibited no behaviors that suggested pain (e.g., reduced activity, enhanced startle).

DISCUSSION:

Chondroitinase treatment showed efficacy on both anatomical and functional outcome measures. On functional assays, effects were only suggested on forelimb measures (which were anatomically targeted by Chase injections into cervical segments mediating hand control), whereas effects were not evident on hindlimb measures. Anatomically, Chase treatment significantly increased the length of corticospinal axons in cervical spinal cord segments below the lesion, representing sprouting of axons spared by the lesion, and also significantly increased the number of corticospinal terminals co-localizing with a synaptic marker, indicating a likely increase in the number of corticospinal synapses.

In contrast to studies in rats and cats [24], effects of Chase on serotonergic axons were not detected. Interestingly, serotonergic axons do not detectably sprout following C7 hemisection lesions in rhesus monkeys [30,39]. A number of mechanisms could potentially account for this observation, including the possibility that serotonergic axons are highly branched and sustaining collaterals may minimize injury responses in the hemisection model [46].

The overall functional success of food object retrieval on the Brinkman board task, a test of finger use, was 47 ± 12% among Chase-injected animals compared to 31 ± 14% in lesioned controls. Chase-treated subjects also showed better recovery than lesioned controls on an object manipulation scale in the testing enclosure (21.25 pt. improvement vs. 12.5 pt. improvement; Fig. 3D). On anatomical measures, CST axon terminal innervation was 50% denser after Chase treatment (Fig. 4C) and the number of putative synapses by corticospinal axons increased 2-fold compared to lesioned controls (Fig. 4E). The reticulospinal system was not traced or quantified in this study. It is possible that, like the CST, reticulospinal axons might sprout in response to Chase treatments and mediate functional recovery.

We developed the non-human primate model of SCI to enable testing of potential translational therapies, invasive therapies in particular, prior to human translation. The rhesus monkey represents the most proximate animal model of the human nervous system that is experimentally testable. We have found that rhesus macaques exhibit variation in motivation, task engagement, and response to injury that constitutes a source of variability exceeding that encountered in rodent models. This variability may result from the increased complexity of the rhesus brain compared to the rodent, and/or the considerable genetic differences in primates that exceed variation found even in outbred rat strains. Consequently, it is likely that this non-human primate model, while less variable than human injuries, incorporates some features of the variability typically encountered in the human clinical setting. Thus, the ability to detect significant differences on several measures following Chase administration, despite inter-subject variability in this model, provides support for the initiation of human clinical trials. While the sample size in this study is small, the costs and duration of this work constitute a relative barrier to studying larger numbers of animals. Our use of data-driven multivariate statistical analysis prior to hypothesis testing allowed us to efficiently test recovery in ensemble across multiple tasks, thereby maximizing information gain with small N, while remaining sensitive to therapeutic effects [47]. Notably, multivariate statistics are not typically employed in clinical trials, which instead generally

rely on one or two pre-defined outcome measures to establish clinical efficacy [48]. Interestingly, had we used classical univariate statistics in the present study, the functional benefit of Chase therapy would likely not have been appreciated. This raises the possibility that a treatment of potential functional benefit might be unappreciated in a clinical trial, despite the presence of a clear biological benefit at the level of axonal growth and synaptogenesis. This finding highlights the great importance of continued consideration and development of multivariate outcome measures in clinical trials, a point that is receiving increasing attention [49,50].

There are important limitations to this non-human primate model of SCI. First, the injury itself is a hemisection, rather than a contusion, which is generally considered more representative of human injuries. We have, in fact, developed a contusive model of SCI in the non-human primate, which could be employed in future pre-clinical studies [44]. Second, the C7 level of the hemisection SCI is optimally placed for recovery of hand function. New studies would be required to assess potential benefit to humans with higher cervical injuries or with thoracic injuries, although preceding rat SCI studies have demonstrated functional benefits of Chase after C4 [14,15] and thoracic [16] SCI.

In addition to presenting evidence of efficacy, this study also preliminarily demonstrates that multiple parenchymal injections of Chase appear to be well-tolerated. The outcome of the present study, taken together with beneficial effects observed by many independent research groups in various rodent models of SCI, support the concept of translation of Chase treatment to human clinical trials.

The large-animal porcine model revealed that intrathecal infusions of the native Chase enzyme at even relatively high concentrations did not reach gray matter target regions. Thus, to advance these proof-of-concept studies into the clinically-relevant primate model of SCI, we turned to more invasive intraparenchymal injections of Chase. The injections appeared to be well-tolerated anatomically based on inflammatory markers and cell counts. Chemical modifications to Chase may enhance its penetrant properties after intrathecal administration, a possibility that merits further study for potential future clinical translation.

Methods:

Subjects

We studied a total of 14 rhesus macaques (*Macaca mulatta*, male, aged 6–10 years) and seven pigs (American Yorkshire-Landrace-Duroc pigs, male, aged 4–6 months). Power analysis: two of the macaques were utilized to establish the delivery efficacy of intraparenchymal Chase administration. The remaining 12 macaques were split into two groups of 6. At a standard deviation of 20% (an estimate drawn from our previous work) and effect size of 40%, N=6 per group gives a computed power of 0.89 at an alpha level of 0.05. Power analyses were not performed for the porcine preliminary study of intrathecal Chase delivery. All surgical and experimental procedures adhered to the principles outlined by American Association for the Accreditation of Laboratory Animal Care. Porcine subjects were housed and tested at MPI, Inc., which is USDA registered and compliant with the Animal Welfare Act (AWA), and has Assurance of Compliance with the Public Health

Service Policy for the Humane Care and Use of Laboratory Animals (PHS/OLAW Assurance). Non-human primates were housed and surgeries performed at the California National Primate Research Center (CNPRC, Davis, CA); all primate procedures were approved by the CNPRC Institutional Animal Care and Use Committee (IACUC). Subsequent tissue processing and analysis was performed at the Center for Neural Repair (University of California, San Diego; La Jolla, CA) or at Cambridge University.

Porcine Study

Spinal cord lesions were not made. All subjects underwent intrathecal catheter placement at T11–13 and Chase provided by Acorda was infused through this indwelling catheter every other day for a total of 14 days (7 doses). Subjects were transcardially perfused two days later. Subjects were randomly assigned to one of 3 groups: one animal received saline only (2 ml per infusion), three animals received low-dose Chase (5 Units/ml × 2 ml per infusion, total dose over 14 days of 70 Units), and three animals received high-dose Chase (25 Units/ml × 2 ml per infusion, total dose over 14 days of 350 Units). Note that because Chase is an enzyme, it is packaged and administered according to units of enzymatic activity (U). For Chase, 1 U is the amount that catalyzes the conversion of 1 micro-mole of chondroitin sulfate A or C per minute at 37°C and pH 8.0. The low dose was comparable to rat intrathecal studies, scaled according to CSF volume. The high dose was meant to test whether better CSPG degradation could be achieved with higher Chase concentration, but showed no difference in CSPG degradation compared to the low dose (see Results). Subjects were sacrificed 2 days after the last infusion (16 days after the first infusion). Because Chase achieves its maximum digestion range within 24 hours [51,52], this time point should reflect the extent of CSPG digestion achievable through intrathecal administration. Spinal cords with dura intact were removed, sectioned into 1 cm blocks and fixed in 4% cold paraformaldehyde for 24 hours. Tissue was transferred to 10% glycerol/2% DMSO in PBS overnight and then transferred to 20% glycerol/ 2% DMSO in PBS (pH 7.4) and was stored refrigerated (2 to 8°C). Tissue was sent to UCSD and sectioned in the coronal plane on a freezing microtome set at 35μm intervals. Sections were then labeled as detailed below for primate studies.

Primate Lesion Surgery

Animals were sedated with 1 mg/kg ketamine intramuscularly and anesthetized with 1.5–2.5% isoflurane. The caudal half of the C5 dorsal lamina and the entire C6 dorsal lamina were removed. The dura was slit longitudinally along the midline and retracted gently. A surgical micro-knife was mounted on a stereotaxic arm positioned at the spinal midline midway between the C5 and C6 dorsal laminae. This rostrocaudal position corresponds to the C7 spinal cord segment. The stereotaxic manipulator was used to lower the blade through the entire dorsoventral extent of the spinal cord without severing the ventral artery. This initial cut established the medial position of the lesion. The lesion was then completed using microscissors under microscopic observation by the surgeon to ensure lesion completeness laterally and ventrally. The dura was sutured, then the overlying muscle and skin were sutured in layers. Animals retained bowel, bladder, and autonomic function after SCI. Lesion reconstructions are shown in Suppl. Fig. 7.

Chondroitinase Injections

Subjects were assigned to Chase-treated or control groups according to post-lesion performance on functional tests (see below) such that pre-treatment functional deficits were equivalent across groups. Four weeks after SCI, the lesion site was re-exposed, and additional laminectomy and longitudinal dural incision was performed to expose the C7–C8-T1 spinal cord. Hand-assembled nested silica cannulae (240 and 150 μm outside diameter, www.molex.com) were attached to a NanoFil 100 μl syringe (www.wpiinc.com) filled with 20 U/ml chondroitinase ABC (a gift of Acorda Therapeutics, Ardsley, New York) in ice-cold saline solution. This concentration of Chase is at the higher end of the spectrum of doses used in the literature [10,17,24,53–56]. Because Chase is an enzyme, it tends to be active upon reaching a threshold activity concentration, and higher concentrations are typically ineffective in generating a greater effect [10,17,24,53–56]. The volume injected (5 μl per site) was scaled from previous rat studies according to spinal cord cross-sectional area (monkey ~= 10× rat). The syringe was mounted in a syringe pump attached to a stereotaxic frame. 5 μl of chondroitinase was injected into the spinal cord parenchyma at each of 10 sites caudal to the SCI site. The first site was 1 mm caudal to the lesion border, each additional site was 1.5 mm further caudal. Each site was 0.7 mm medial to the medial edge of the dorsal root entry zone (DREZ) on the right side of the spinal cord. At each site, the pia was nicked with a 25G needle to allow cannula entry. Chondroitinase was injected at two depths (2.5 mm and 3.5 mm; 2.5 μl each) at a rate of 0.5 μl/min. To minimize Chase reflux, after the second injection at each site we waited 2 min before withdrawing the cannula. As with the initial SCI, the dura was sutured, then the overlying muscle and skin were sutured in layers. No adverse effects were observed following Chase administration.

Corticospinal tracing

CST axons were traced to assess regeneration into the graft. As previously described [45], six weeks prior to sacrifice (4 months after SCI), the subject was anesthetized and a craniotomy was performed to expose the right and left motor cortex. Using a pulled glass micropipette attached to a picospritzer (Parker Hannifin, Fairfield, NJ), 300 nl of the anterograde neuronal tracer biotinylated dextran amine (BDA; 10,000 MW, 10% in water, Thermo Fisher) was injected at each of 127 sites (59 different surface locations) in the left motor cortex. These sites included motor cortex innervating the hand, arm, trunk, leg, and foot. Identical injections of the anterograde tracer dextran-conjugated Alexa Fluor-488 (A488, 10,000 MW, 5% in water, Thermo Fisher) were made in the right motor cortex. After tracer injection, the excised piece of cranium was replaced, cemented in place with dental acrylic, and the incision closed in layers.

Tissue processing

Subjects were sacrificed 5.5 months after SCI. Subjects were deeply anesthetized and transcardially perfused with a 4% solution of paraformaldehyde, and the spinal cord was dissected out of the spinal column. Spinal cord dura was removed, and the spinal cord was cut in the transverse plane into 1.5-cm-long blocks as detailed previously [30]. Blocks from segments C3, C7, C8, T1, and T2 were cut into 40-μm-thick transverse sections using a

freezing microtome. Tissue sections were stored at −20 °C in cryoprotectant (25% glycerin (v/v), 30% ethylene glycol (v/v) in 0.05 M phosphate buffer).

Fluorescent immunolabeling

Transverse sections were pre-treated with 50% methanol for 20 min at 22–24°C, washed in tris-buffered saline (TBS) and blocked for 1 hr in TBS containing 5% normal donkey serum and 0.25% Triton X-100. Sections were incubated in streptavidin 488 (1:400, Life Tech) and/or primary antibodies against serotonin (1:5000, Immunostar), synaptophysin (1:300, Sigma), IBA1 (1:1500, Wako), GFAP (1:1500, Encor Bio). Sections were washed with TBS and then incubated in Alexa-Fluor 488- or 594-conjugated secondary antibodies (Thermo Fisher, 1:500) for 1 hour. Sections were washed with TBS, mounted on slides, and coverslipped with Mowiol mounting medium (http://cshprotocols.cshlp.org/content/2006/1/pdb.rec10255). All antibodies were used previously in monkeys [30].

Light-level labeling

For WFA and BDA detection, sections were washed in TBS and then quenched in 0.6% H2O2 in 50% methanol in TBS for 30 minutes. Sections were then washed with TBS and incubated overnight at 4°C in WFA-biotin (1:1000; reduced form; Sigma L1766) or Vectastain Elite ABC solution (Vector Labs) and 0.25% Triton-X100 in TBS. WFA sections were washed with TBS, then incubated with Vectastain Elite ABC solution for 1 hour. All sections were then washed again and developed with diaminobenzidine (DAB) and NiCl2. Sections were mounted on gelatin-subbed glass slides, dehydrated, and coverslipped with DPX mounting medium.

For A488, CD8, CD3, and CD45 detection, sections were washed in TBS and then quenched in 0.6% H2O2 in 100% methanol in TBS for 30 minutes. Sections were then washed with TBS, blocked for 1 hr in 5% horse serum and 0.25% Triton-X100 in TBS (TBS++), and incubated at 4°C in TBS++ with rabbit anti-A488 (1:5000, ThermoFisher) for two nights, or mouse anti-CD8 (1:500, BD Pharmingen), mouse anti-CD3 (1:500, BD Pharmingen), or mouse anti-CD45 (1:500, BD Pharmingen) for one night. Sections were washed in TBS, then incubated for 45 minutes in, as appropriate, horse-anti-rabbit or horse-anti-mouse Vector ImmPRESS (1:1, Vector Labs) in TBS. Sections were washed again and developed with DAB and NiCl2. Sections were mounted on gelatin-subbed glass slides, dehydrated, and coverslipped with DPX mounting medium.

For 2B6 detection, pig tissue sections were washed in TBS and then quenched in 0.6% H2O2 in TBS for 30 minutes. Sections were then washed with TBS, blocked for 1 hr in 5% horse serum and 0.25% Triton-X100 in TBS (TBS++), and incubated at 4°C in TBS++ with mouse anti-2B6 (1:2000, Seikagaku, now available from Amsbio) for one night. Sections were washed in TBS, then incubated for 1 hour in biotinylated horse-anti-mouse IgG (1:200, Vector) in TBS++. Sections were washed again with TBS, then incubated with Vectastain Elite ABC solution for 45 minutes. Sections were then washed again and developed with diaminobenzidine (DAB) and NiCl2. Sections were mounted on gelatin-subbed glass slides, dehydrated, and coverslipped with DPX mounting medium.

Nissl substance was labeled in sections from a 1:12 series covering spinal cord segments C3, C7, C8, T1, and T2. Sections were washed in TBS, fixed in buffered 4% paraformaldehyde for 1 hour at room temperature, mounted on gelatin-subbed glass slides, and dried overnight. Sections were then defatted in a 1:1 mixture of chloroform and ethanol, rehydrated, placed briefly in 0.25% thionin, dehydrated, cleared, and coverslipped.

Quantification of axons, synapses, motor neurons, microglia

Axon density was quantified with ImageJ 1.41c (Wayne Rasband, National Institutes of Health, rsb.info.nih.gov/ij/) and a custom-written script (J.J.L.), derived from previous methods (E.S.R.)[30]. 20× images of the entire spinal cord were obtained, and loaded into ImageJ. All images were corrected for brightness and contrast equally to reduce background noise. For CST axons, regions of interest (ROIs) were drawn around the right gray matter. For 5HT-labeled raphespinal axons, ROIs were drawn around the right and left motor pools. The image was auto-thresholded, the detected fiber profiles were skeletonized (so that sum of pixels = total axon length) and measurements for each ROI were recorded in the right gray matter.

Synapse counts (colocalization of BDA and synaptophysin) were performed with 60× confocal image stacks loaded into ImageJ. Three non-overlapping image stacks were obtained in the right IZ of each of 4 tissue sections per subject. The experimenter systematically sampled the entire image stack for clearly co-localized BDA and Syn in bouton-like swellings connected to BDA-labeled axons. The number of putative synapses was divided by the volume of the image stack (~900,000 μm^3) and converted to synapses/mm^3.

Spinal motor neurons (MNs) were counted in Nissl-labeled sections at sequential rostro-caudal distances from a sample injection site on both injected and uninjected sides of the spinal cord. The number of MNs on the injected side was divided by the sum of the number of MNs on injected and uninjected sides, such that the expected proportion was 0.5. Five to six total sections were counted per subject (up to one section per x-axis position).

Microglial density was quantified using IBA1 labeling. IBA1 pixel density was calculated using the ImageJ autothresholding function on images of the intermediate zone of the gray matter in tissue sections immediately adjacent to injection sites (or similar regions in C8–T1 spinal cord for uninjected subjects). Tissue sections from subjects in the present experiment were immunolabeled for IBA1 concurrently with sections from subjects involved in a previous study ([30]; N=3 Intact subjects, N=4 subjects 2 weeks after C7 hemisection SCI, N=3 subjects 5 months after C7 hemisection SCI);

Experimenters were blind to group membership during all quantitative analyses.

Functional testing

Functional outcomes were assessed in an open-field paradigm using an ordinal scale, as described in detail in [42,44]. In the open-field testing enclosure ($5 \times 7 \times 10 ft^3$), monkeys can access perches at various levels, climb along the enclosure walls, and manipulate objects containing small food rewards using dexterous hand movements. Use of each hindlimb and

forelimb on the tasks is rated by an observer over the 30 min observation period; video recordings allow re-assessments as necessary. A total of 72 points on the scale are possible. We also rated monkeys on a 22-point forelimb subscore that focuses on arm, hand and digit use during object manipulation [42,44]. Monkeys underwent pre-lesion baseline training, followed by three half hour exposures per week to the enclosure to encourage activity and limb use. Performance was videotaped and rated once weekly. We compared the level of functional performance of lesioned control monkeys (N=5) to Chase-treated monkeys (N=6).

Subjects' ability to perform fine motor functions with the affected hand were also assessed using a modified, cage-mounted Brinkman board, which requires use of the affected (right) hand to retrieve small food items. This custom-made plexiglas box is hung at the front of each animal's cage. The left hand pushes a spring-mounted lever, which moves a plexiglas occlusion plate, giving the affected hand access to the Brinkman board under the occlusion plate. This configuration allows the subject to perform the task in the home cage, and requires use of the affected hand, ensuring optimal rehabilitation and functional testing. Five different boards of increasing difficulty were presented sequentially in each testing session. Difficulty is increased by: 1) increasing the depth of wells from which monkeys need to extract the food reward, 2) altering the angle of the well relative to the monkey's position, and 3) increasing the number of reward wells (Fig. 3). Monkeys were scored on the number of rewards obtained from each board, the time to clear the board, and whether a pincer grasp was used.

All functional outcomes were measured and recorded by observers blinded to treatment group.

Statistical Analysis

For statistical analysis of functional data, we employed an *a priori* established, blinded, data-driven statistical workflow, (Suppl. Fig. 11; [57]). Diagnostic analyses of raw ordinal data revealed non-normal and non-parametric features across measures; thus, non-parametric and non-linear statistical tests were used throughout. Analysis was divided into two distinct stages. First, we compiled the full behavioral data outcome matrix (animals × tests × time points) and performed non-linear PCA (NLPCA) on whole matrix from all animals (both treated and untreated). The PC loadings were then examined and cross-validated to confirm the resulting PC scores serve as legitimate multidimensional outcome metrics [58–60]. This was done in a computationally unsupervised manner by applied biostatisticians (JRH, ARF) blind to experimental condition. Second, we performed a directed, single hypothesis test (linear mixed model, Figure 3A), unblinded to the effect of Chase on PC1. This staged statistical analysis approach brings together machine-learning-based pattern detection (stage 1), with hypothesis testing (stage 2) to maximize outcome information without relying on multiple hypothesis testing, thereby limiting the statistical false discovery rate. Technically, the NL-PCA approach (stage 1) reduces the large amount of behavioral data (open-field and each level of brinkman board for each animal at each timepoint) into an overall integrated behavioral score, while taking into account level of measurement of each measure (ordinal, continuous, etc.) and a wide range of possible distributions, through optimal scaling

transformations and pattern detection using the alternating least squares algorithm [61]. The resulting principal components are orthogonal and, by definition, normally distributed, with the first PC accounting for the most variance. The PC loading reflects the correlation between each measure and the non-linear PC. The squared factor loading for each of these measures indicates the percentage of variance in a principal component that is explained by that measure. A bootstrapping procedure was then used for internal validation of the loading pattern. The bootstrapping procedure is a nonparametric approach that resampled the dataset 1,000 times, with each iteration producing loadings from a slight variation of the original dataset. This step was followed by a pattern matching algorithm to test the similarity between the original and bootstrapped loading patterns. After confirmation of loading pattern stability, PC loading weights were then applied to derive a PC score for each animal at each individual time-point. In stage 2, we applied a linear mixed model (LMM) to assess the impact of chase on PC scores over time for each group, using a diagonal covariance matrix structure with individual animal as a random factor, thereby standardizing scores for each animal according to their pre-drug baseline function. Stage 1 and stage 2 were implemented in IBM SPSS Statistics v.25 using CATPCA and LMM subcommands, respectively. Repeated measures analysis of variance (ANOVA) was used to test for main effects of time for each group in instances where data had no missing values, with sphericity assumed. CST and synapse measurements were also analyzed using an LMM, with histological section set as a repeated measure for each subject, using a diagonal covariance matrix structure and subject as a random factor. A generalized estimating equation (GEE) model was used for non-linear 5HT ratio data. Linear mixed models and GEEs are modern approaches that do not suffer from the violations of ‘independence’ and ‘sphericity’ assumptions that plague general linear modeling approaches popularized in the 20th century [62]. Given that the linear mixed model procedure is not bound by the assumptions of equal variance and does not assume repeated measures are independent, the ability to model both fixed and random effects in one model thus allows for the variance (and covariance of repeated measures)to be *modeled* rather than assumed to be equal. For linear mixed model procedures, the covariance matrix was specified by the structure that best fit the data as determined by Akaike information criteria (AIC). F values and degrees of freedom are reported for all ANOVA and LMM (precise, fractional df reported) and Wald Chi squared value is reported for the GEE model. Effect sizes and fit metrics for each analysis are reported throughout (partial eta squared (η_p^2) for F tests, AIC for linear mixed models, quasi-likelihood under the independence model criterion (QIC) for GEE). As main effects were between only two conditions throughout, no post hoc corrections for multiple comparisons were necessary. Statistical significance for all effects was assessed at a p value below 0.05. All analyses were run using SPSS v.25 (IBM).

Life Sciences Reporting Summary

Additional details on experimental design and reagents are available in the Life Sciences Reporting Summary, published alongside this paper.

Data Availability

The data that support the findings of this study are available from the corresponding author upon reasonable request. The custom-written ImageJ scripts are also available from the corresponding author upon reasonable request.

Supplementary Material

Refer to Web version on PubMed Central for supplementary material.

ACKNOWLEDGMENTS:

This work was supported by the National Institutes of Health (NS042291, MHT) and Acorda Therapeutics, Inc. Core infrastructure support for the primate spinal cord research facility was provided by the Veterans Administration (Gordon Mansfield Spinal Cord Injury Collaborative Consortium IP50RX001045, RR&D B7332R, MHT; RR&D 1I01RX002245, ARF). The California National Primate Research Center is funded by the NIH (NCRR P51 OD011107–56). Funding was also provided by the Craig H. Neilsen Foundation (MHT), the Bernard and Anne Spitzer Charitable Trust (MHT), the Dr. Miriam and Sheldon G. Adelson Medical Research Foundation (MHT), the British Medical Research Council (JWF), and the Christopher and Dana Reeve Foundation (JWF).

REFERENCES:

1. Schwab ME. Nogo and axon regeneration. Curr. Opin. Neurobiol 2004;14:118–24. [PubMed: 15018947]
2. Fitch MT, Silver J. CNS injury, glial scars, and inflammation: Inhibitory extracellular matrices and regeneration failure. Exp. Neurol 2008;209:294–301. [PubMed: 17617407]
3. Kwok JCF, Afshari F, García-Alías G, Fawcett JW. Proteoglycans in the central nervous system: plasticity, regeneration and their stimulation with chondroitinase ABC. Restor. Neurol. Neurosci 2008;26:131–45. [PubMed: 18820407]
4. Tran AP, Warren PM, Silver J. The Biology of Regeneration Failure and Success After Spinal Cord Injury. Physiol. Rev 2018;98:881–917. [PubMed: 29513146]
5. Dou CL, Levine JM. Inhibition of neurite growth by the NG2 chondroitin sulfate proteoglycan. J. Neurosci 1994;14:7616–28. [PubMed: 7996200]
6. Levine JM, Nishiyama A. The NG2 chondroitin sulfate proteoglycan: a multifunctional proteoglycan associated with immature cells. Perspect. Dev. Neurobiol 1996;3:245–59. [PubMed: 9117258]
7. Jones LL, Yamaguchi Y, Stallcup WB, Tuszynski MH. NG2 Is a Major Chondroitin Sulfate Proteoglycan Produced after Spinal Cord Injury and Is Expressed by Macrophages and Oligodendrocyte Progenitors. J. Neurosci 2002;22:2792–803. [PubMed: 11923444]
8. Grimpe B, Silver J. A Novel DNA Enzyme Reduces Glycosaminoglycan Chains in the Glial Scar and Allows Microtransplanted Dorsal Root Ganglia Axons to Regenerate beyond Lesions in the Spinal Cord. J. Neurosci 2004;24:1393–7. [PubMed: 14960611]
9. Wang D, Fawcett J. The perineuronal net and the control of CNS plasticity. Cell Tissue Res 2012;349:147–60. [PubMed: 22437874]
10. Alilain WJ, Horn KP, Hu H, Dick TE, Silver J. Functional regeneration of respiratory pathways after spinal cord injury. Nature 2011;475:196–200. [PubMed: 21753849]
11. Filous AR, Tran A, Howell CJ, Busch SA, Evans TA, Stallcup WB, Kang SH, Bergles DE, Lee S, Levine JM, Silver J. Entrapment via Synaptic-Like Connections between NG2 Proteoglycan+ Cells and Dystrophic Axons in the Lesion Plays a Role in Regeneration Failure after Spinal Cord Injury. J. Neurosci 2014;34:16369–84. [PubMed: 25471575]
12. Lang BT, Cregg JM, DePaul MA, Tran AP, Xu K, Dyck SM, Madalena KM, Brown BP, Weng Y-L, Li S, Karimi-Abdolrezaee S, Busch SA, Shen Y, Silver J. Modulation of the proteoglycan receptor PTPσ promotes recovery after spinal cord injury. Nature 2015;518:404–8. [PubMed: 25470046]

13. Moon LD, Asher RA, Rhodes KE, Fawcett JW. Regeneration of CNS axons back to their target following treatment of adult rat brain with chondroitinase ABC. Nat. Neurosci 2001;4:465–6. [PubMed: 11319553]
14. Bradbury EJ, Moon LDF, Popat RJ, King VR, Bennett GS, Patel PN, Fawcett JW, McMahon SB. Chondroitinase ABC promotes functional recovery after spinal cord injury. Nature 2002;416:636–40. [PubMed: 11948352]
15. García-Alías G, Barkhuysen S, Buckle M, Fawcett JW. Chondroitinase ABC treatment opens a window of opportunity for task-specific rehabilitation. Nat. Neurosci 2009;12:1145–51. [PubMed: 19668200]
16. Caggiano AO, Zimber MP, Ganguly A, Blight AR, Gruskin EA. Chondroitinase ABCI improves locomotion and bladder function following contusion injury of the rat spinal cord. J. Neurotrauma 2005;22:226–39. [PubMed: 15716629]
17. Galtrey CM, Asher RA, Nothias F, Fawcett JW. Promoting plasticity in the spinal cord with chondroitinase improves functional recovery after peripheral nerve repair. Brain 2007;130:926–39. [PubMed: 17255150]
18. Starkey ML, Bartus K, Barritt AW, Bradbury EJ. Chondroitinase ABC promotes compensatory sprouting of the intact corticospinal tract and recovery of forelimb function following unilateral pyramidotomy in adult mice. Eur. J. Neurosci 2012;36:3665–78. [PubMed: 23061434]
19. Houle JD, Tom VJ, Mayes D, Wagoner G, Phillips N, Silver J. Combining an Autologous Peripheral Nervous System “Bridge” and Matrix Modification by Chondroitinase Allows Robust, Functional Regeneration beyond a Hemisection Lesion of the Adult Rat Spinal Cord. J. Neurosci 2006;26:7405–15. [PubMed: 16837588]
20. James ND, Shea J, Muir EM, Verhaagen J, Schneider BL, Bradbury EJ. Chondroitinase gene therapy improves upper limb function following cervical contusion injury. Exp. Neurol 2015;271:131–5. [PubMed: 26044197]
21. Soleman S, Yip PK, Duricki DA, Moon LDF. Delayed treatment with chondroitinase ABC promotes sensorimotor recovery and plasticity after stroke in aged rats. Brain 2012;135:1210–23. [PubMed: 22396394]
22. Hill JJ, Jin K, Mao XO, Xie L, Greenberg DA. Intracerebral chondroitinase ABC and heparan sulfate proteoglycan glypican improve outcome from chronic stroke in rats. Proc. Natl. Acad. Sci. U. S. A 2012;109:9155–60. [PubMed: 22615373]
23. Gherardini L, Gennaro M, Pizzorusso T. Perilesional treatment with chondroitinase ABC and motor training promote functional recovery after stroke in rats. Cereb. Cortex 2015;25:202–12. [PubMed: 23960208]
24. Tester NJ, Howland DR. Chondroitinase ABC improves basic and skilled locomotion in spinal cord injured cats. Exp. Neurol 2008;209:483–96. [PubMed: 17936753]
25. Mondello SE, Jefferson SC, Tester NJ, Howland DR. Impact of treatment duration and lesion size on effectiveness of chondroitinase treatment post-SCI. Exp. Neurol 2015;267:64–77. [PubMed: 25725355]
26. Ginsberg MD. Neuroprotection for ischemic stroke: Past, present and future. Neuropharmacology 2008;55:363–89. [PubMed: 18308347]
27. Howells DW, Sena ES, Macleod MR. Bringing rigour to translational medicine. Nat. Rev. Neurol 2014;10:37–43. [PubMed: 24247324]
28. Schumacher M, Denier C, Oudinet J-P, Adams D, Guennoun R. Progesterone neuroprotection: The background of clinical trial failure. J. Steroid Biochem. Mol. Biol 2016;160:53–66. [PubMed: 26598278]
29. Tator CH. Review of treatment trials in human spinal cord injury: issues, difficulties, and recommendations. Neurosurgery 2006;59:957–82. [PubMed: 17143232]
30. Rosenzweig ES, Courtine G, Jindrich DL, Brock JH, Ferguson AR, Strand SC, Nout YS, Roy RR, Miller DM, Beattie MS, Havton LA, Bresnahan JC, Edgerton VR, Tuszynski MH. Extensive spontaneous plasticity of corticospinal projections after primate spinal cord injury. Nat. Neurosci 2010;13:1505–10. [PubMed: 21076427]
31. Lawrence DG, Kuypers HG. The functional organization of the motor system in the monkey. I. The effects of bilateral pyramidal lesions. Brain J. Neurol 1968;91:1–14.

32. Hepp-Reymond MC, Trouche E, Wiesendanger M. Effects of unilateral and bilateral pyramidotomy on a conditioned rapid precision grip in monkeys (Macaca fascicularis). Exp. Brain Res 1974;21:519–27. [PubMed: 4442500]
33. Bunge RP, Puckett WR, Becerra JL, Marcillo A, Quencer RM. Observations on the pathology of human spinal cord injury. A review and classification of 22 new cases with details from a case of chronic cord compression with extensive focal demyelination. Adv. Neurol 1993;59:75–89. [PubMed: 8420126]
34. Kakulas BA. A review of the neuropathology of human spinal cord injury with emphasis on special features. J. Spinal Cord Med 1999;22:119–24. [PubMed: 10826269]
35. Nout YS, Rosenzweig ES, Brock JH, Strand SC, Moseanko R, Hawbecker S, Zdunowski S, Nielson JL, Roy RR, Courtine G, Ferguson AR, Edgerton VR, Beattie MS, Bresnahan JC, Tuszynski MH. Animal models of neurologic disorders: a nonhuman primate model of spinal cord injury. Neurotherapeutics 2012;9:380–92. [PubMed: 22427157]
36. Weidner N, Ner A, Salimi N, Tuszynski MH. Spontaneous corticospinal axonal plasticity and functional recovery after adult central nervous system injury. Proc. Natl. Acad. Sci. U. S. A 2001;98:3513–8. [PubMed: 11248109]
37. Brus-Ramer M, Carmel JB, Chakrabarty S, Martin JH. Electrical stimulation of spared corticospinal axons augments connections with ipsilateral spinal motor circuits after injury. J. Neurosci 2007;27:13793–801. [PubMed: 18077691]
38. Ghosh A, Sydekum E, Haiss F, Peduzzi S, Zörner B, Schneider R, Baltes C, Rudin M, Weber B, Schwab ME. Functional and anatomical reorganization of the sensory-motor cortex after incomplete spinal cord injury in adult rats. J. Neurosci 2009;29:12210–9. [PubMed: 19793979]
39. Friedli L, Rosenzweig ES, Barraud Q, Schubert M, Dominici N, Awai L, Nielson JL, Musienko P, Nout-Lomas Y, Zhong H, Zdunowski S, Roy RR, Strand SC, van den Brand R, Havton LA, Beattie MS, Bresnahan JC, Bézard E, Bloch J, Edgerton VR, Ferguson AR, Curt A, Tuszynski MH, Courtine G. Pronounced species divergence in corticospinal tract reorganization and functional recovery after lateralized spinal cord injury favors primates. Sci. Transl. Med 2015;7:302ra134.
40. Liu K, Lu Y, Lee JK, Samara R, Willenberg R, Sears-Kraxberger I, Tedeschi A, Park KK, Jin D, Cai B, Xu B, Connolly L, Steward O, Zheng B, He Z. PTEN deletion enhances the regenerative ability of adult corticospinal neurons. Nat. Neurosci 2010;13:1075–81. [PubMed: 20694004]
41. Lee JK, Geoffroy CG, Chan AF, Tolentino KE, Crawford MJ, Leal MA, Kang B, Zheng B. Assessing spinal axon regeneration and sprouting in Nogo-, MAG-, and OMgp-deficient mice. Neuron 2010;66:663–70. [PubMed: 20547125]
42. Nout YS, Ferguson AR, Strand SC, Moseanko R, Hawbecker S, Zdunowski S, Nielson JL, Roy RR, Zhong H, Rosenzweig ES, Brock JH, Courtine G, Edgerton VR, Tuszynski MH, Beattie MS, Bresnahan JC. Methods for functional assessment after C7 spinal cord hemisection in the rhesus monkey. Neurorehabil. Neural Repair 2012;26:556–69. [PubMed: 22331214]
43. Shank CD, Walters BC, Hadley MN. Management of acute traumatic spinal cord injuries. Handb. Clin. Neurol 2017;140:275–98. [PubMed: 28187803]
44. Salegio EA, Bresnahan JC, Sparrey CJ, Camisa W, Fischer J, Leasure J, Buckley J, Nout-Lomas YS, Rosenzweig ES, Moseanko R, Strand S, Hawbecker S, Lemoy M-J, Haefeli J, Ma X, Nielson JL, Edgerton VR, Ferguson AR, Tuszynski MH, Beattie MS. A Unilateral Cervical Spinal Cord Contusion Injury Model in Non-Human Primates (Macaca mulatta). J. Neurotrauma 2016;33:439–59. [PubMed: 26788611]
45. Rosenzweig ES, Brock JH, Culbertson MD, Lu P, Moseanko R, Edgerton VR, Havton LA, Tuszynski MH. Extensive spinal decussation and bilateral termination of cervical corticospinal projections in rhesus monkeys. J. Comp. Neurol 2009;513:151–63. [PubMed: 19125408]
46. Leanza G, Perez S, Pellitteri R, Russo A, Stanzani S. Branching serotonergic and non-serotonergic projections from caudal brainstem to the medial preoptic area and the lumbar spinal cord, in the rat. Neurosci. Lett 1995;200:5–8. [PubMed: 8584265]
47. Haefeli J, Ferguson AR, Bingham D, Orr A, Won SJ, Lam TI, Shi J, Hawley S, Liu J, Swanson RA, Massa SM. A data-driven approach for evaluating multi-modal therapy in traumatic brain injury. Sci. Rep 2017;7. [PubMed: 28127057]

48. ICH Harmonised Tripartite Guideline. Statistical principles for clinical trials. International Conference on Harmonisation E9 Expert Working Group. Stat. Med 1999;18:1905–42. [PubMed: 10532877]

49. Rasmussen MA, Colding-Jørgensen M, Hansen LT, Bro R. Multivariate evaluation of pharmacological responses in early clinical trials – a study of rIL-21 in the treatment of patients with metastatic melanoma. Br. J. Clin. Pharmacol 2010;69:379–90. [PubMed: 20406222]

50. Raghavan N, Samtani MN, Farnum M, Yang E, Novak G, Grundman M, Narayan V, DiBernardo A. The ADAS-Cog revisited: Novel composite scales based on ADAS-Cog to improve efficiency in MCI and early AD trials. Alzheimers Dement 2013;9:S21–31. [PubMed: 23127469]

51. García-Alías G, Lin R, Akrimi SF, Story D, Bradbury EJ, Fawcett JW. Therapeutic time window for the application of chondroitinase ABC after spinal cord injury. Exp. Neurol 2008;210:331–8. [PubMed: 18158149]

52. Lin R, Kwok JCF, Crespo D, Fawcett JW. Chondroitinase ABC has a long-lasting effect on chondroitin sulphate glycosaminoglycan content in the injured rat brain. J. Neurochem 2008;104:400–8. [PubMed: 18005340]

53. Hu HZ, Granger N, Pai SB, Bellamkonda RV, Jeffery ND. Therapeutic efficacy of microtube-embedded chondroitinase ABC in a canine clinical model of spinal cord injury. Brain 2018;141:1017–27. [PubMed: 29444239]

54. Iseda T, Okuda T, Kane-Goldsmith N, Mathew M, Ahmed S, Chang Y-W, Young W, Grumet M. Single, high-dose intraspinal injection of chondroitinase reduces glycosaminoglycans in injured spinal cord and promotes corticospinal axonal regrowth after hemisection but not contusion. J. Neurotrauma 2008;25:334–49. [PubMed: 18373483]

55. Jefferson SC, Tester NJ, Howland DR. Chondroitinase ABC Promotes Recovery of Adaptive Limb Movements and Enhances Axonal Growth Caudal to a Spinal Hemisection. J. Neurosci 2011;31:5710–20. [PubMed: 21490212]

56. Steinmetz MP, Horn KP, Tom VJ, Miller JH, Busch SA, Nair D, Silver DJ, Silver J. Chronic Enhancement of the Intrinsic Growth Capacity of Sensory Neurons Combined with the Degradation of Inhibitory Proteoglycans Allows Functional Regeneration of Sensory Axons through the Dorsal Root Entry Zone in the Mammalian Spinal Cord. J. Neurosci 2005;25:8066–76. [PubMed: 16135764]

57. Rosenzweig ES, Brock JH, Lu P, Kumamaru H, Salegio EA, Kadoya K, Weber JL, Liang JJ, Moseanko R, Hawbecker S, Huie JR, Havton LA, Nout-Lomas YS, Ferguson AR, Beattie MS, Bresnahan JC, Tuszynski MH. Restorative effects of human neural stem cell grafts on the primate spinal cord. Nat. Med 2018;24:484–90. [PubMed: 29480894]

58. Linting M, Meulman JJ, Groenen PJF, van der Koojj AJ. Nonlinear principal components analysis: introduction and application. Psychol. Methods 2007;12:336–58. [PubMed: 17784798]

59. Lever J, Krzywinski M, Altman N. Principal component analysis. Nat. Methods 2017;14:641.

60. Ferguson AR, Irvine K-A, Gensel JC, Nielson JL, Lin A, Ly J, Segal MR, Ratan RR, Bresnahan JC, Beattie MS. Derivation of multivariate syndromic outcome metrics for consistent testing across multiple models of cervical spinal cord injury in rats. PloS One 2013;8:e59712. [PubMed: 23544088]

61. Gifi A Nonlinear Multivariate Analysis Wiley; 1990.

62. Cnaan A, Laird NM, Slasor P. Using the general linear mixed model to analyse unbalanced repeated measures and longitudinal data. Stat. Med 1997;16:2349–80. [PubMed: 9351170]

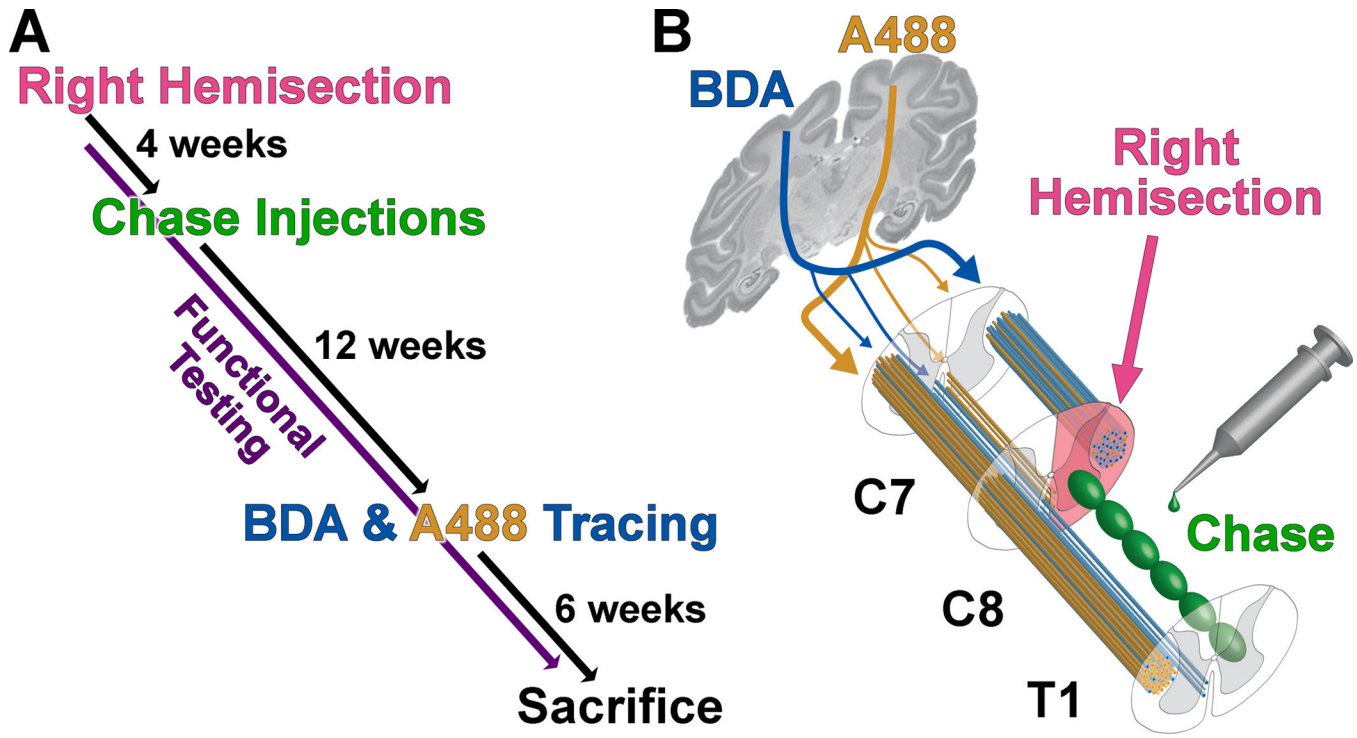

Figure 1: Experimental Approach

(**A**) Timeline of Chase efficacy experiment. (**B**) Schematic of experimental approach. The right hemisection lesion at segment C7 severs 90% of CST axons originating in the left hemisphere (traced with BDA, blue), and 10% of CST axons originating in the right hemisphere (traced with A488, brown). Chase is injected into 10 sites (1.5 mm apart) in the gray matter below the lesion.

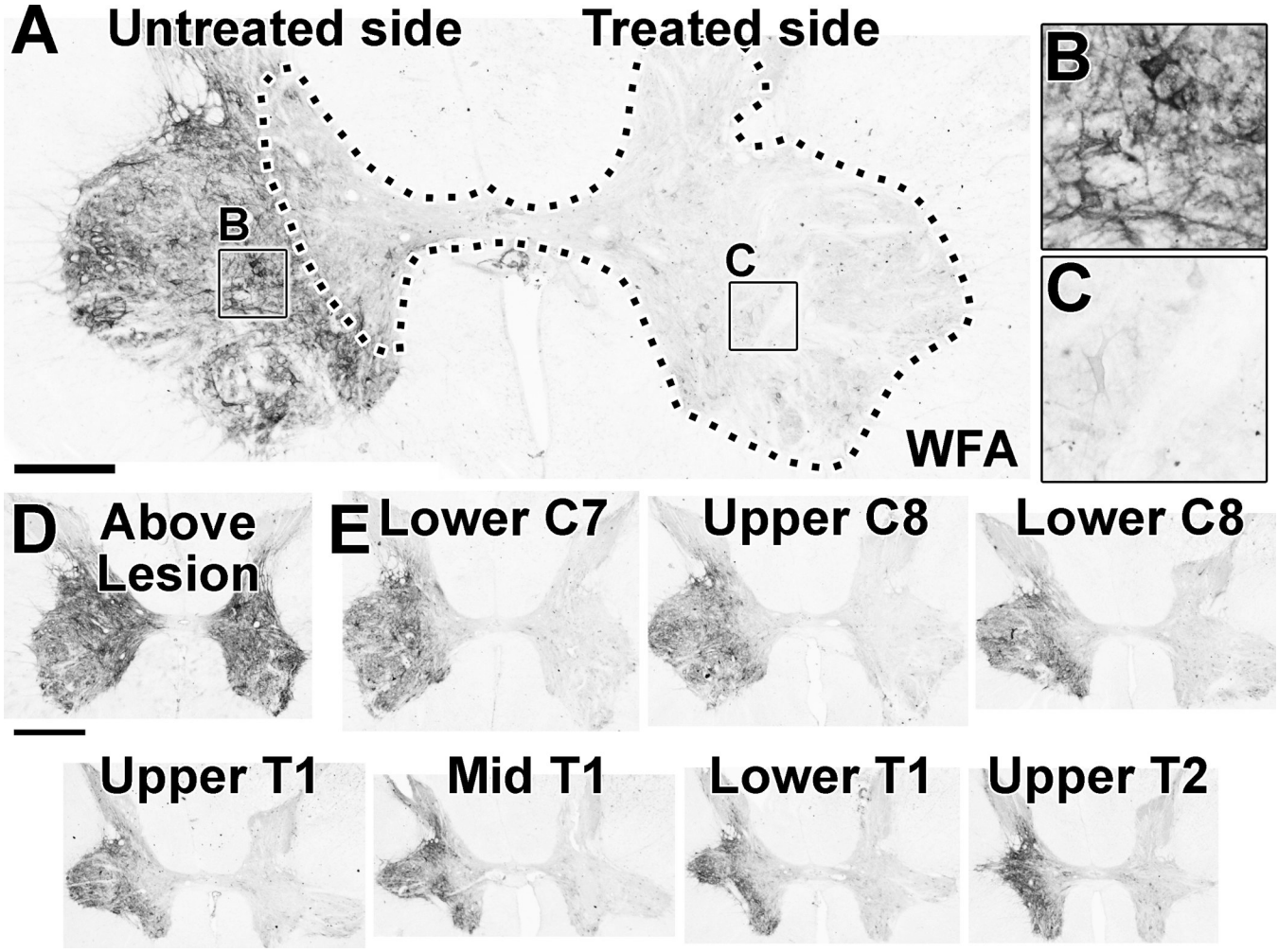

Figure 2: Intraparenchymal Chase Injections Degrade Chondroitin Sulfate Proteoglycans

(**A-C**) Comparison of Chase-treated (right) and untreated (left) sides of the spinal cord in a rhesus monkey 2 wk after Chase administration (1 mo after lesion). WFA labeling reveals CSPG degradation on the treated side. Boxed regions are shown at higher magnification in **B,C**. Zone of peri-neuronal net CSPG degradation indicated by **dashed lines**. (**D**) Tissue section from C7, above the lesion and the treated region, has intact CSPGs. (**E**) Series of tissue sections at 2 mm intervals moving caudally from lesion site reveals effective CSPG degradation from C7 through T1. Labeling experiment included 2 animals. Scale bars: A, 500 μm; B,C, 1 mm.

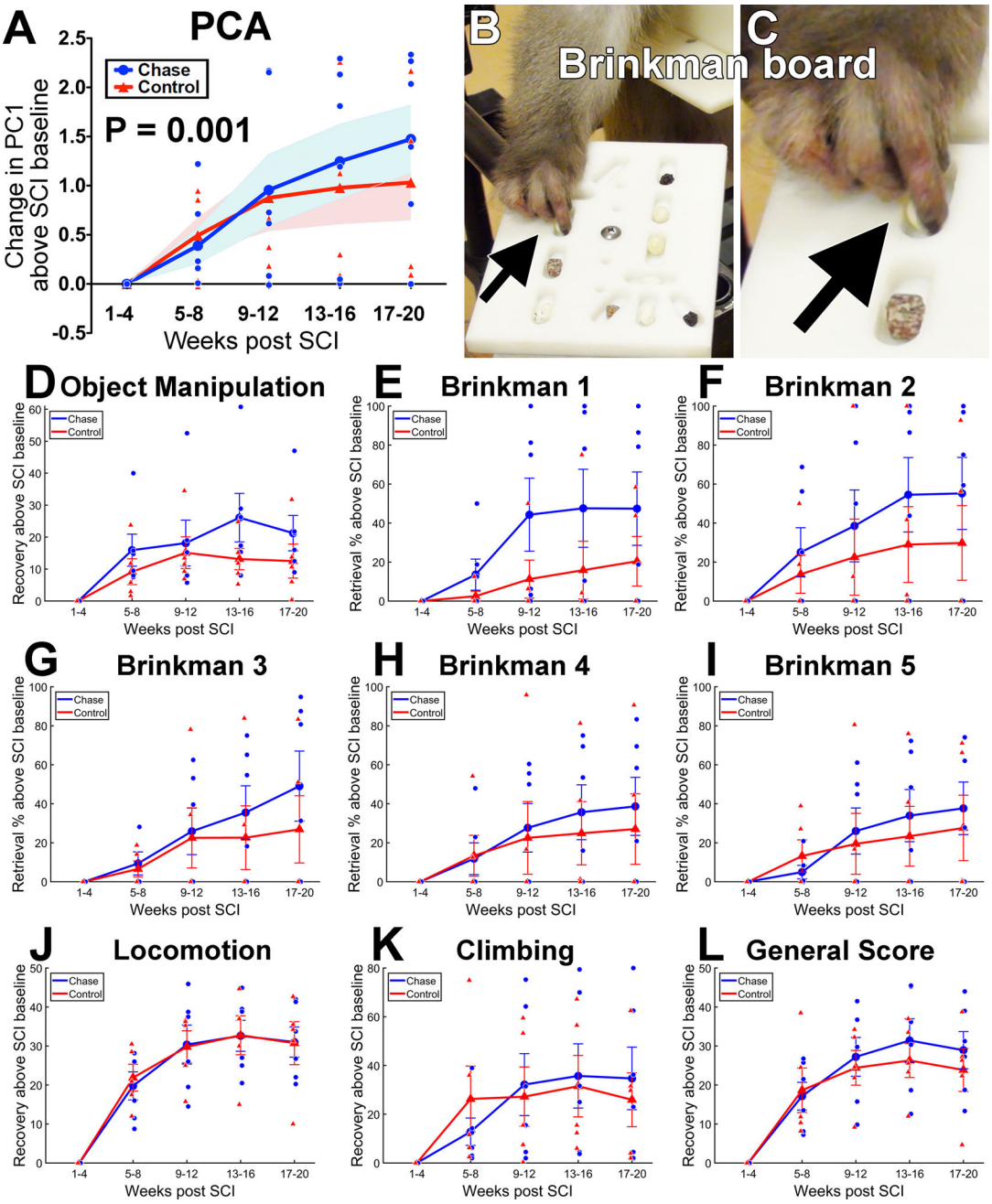

Figure 3: Functional Outcomes

(**A**) Combining all behavioral data into a principal components analysis (PCA) demonstrates a significant interaction of Chase treatment with time on PC1 (LMM, P=0.001). Plot shows the change in PC1 scores over time. Shading represents SEM. PC1 explains 68% of the variance in the behavioral data (see Supp. Fig. 5 for loadings). (**B-C**) Example of food reward retrieval on one of the tasks comprising behavioral testing, Brinkman 5. Arrow indicates pincer motion used to retrieve food reward from well. (**D-L**) Recovery curves for the individual tasks that comprise PC1. These individual task plots show that, although single functional outcome metrics may not be sensitive on their own, combining all metrics

in a PCA reveals a robust effect of chondroitinase treatment at the multivariate level. Object manipulation score (**D**) reflects use of the impaired forelimb to manipulate a large piece of fruit and retrieve food items from inside a “Kong” toy. Brinkman 1 through Brinkman 5 (**E-I**) indicates progressively more difficult versions of food retrieval (see Methods; raw Brinkman scores are reported in the text). Locomotion score (**J**) reflects use of the ipsilesional limbs for moving around the exercise enclosure. (**K**) Climbing score reflects use of ipsilesional limbs for vertical climbing in the exercise enclosure. (**L**) General Score is a composite of multiple measures that describe forelimb and hindlimb function, as described in [42,44]. Generally, the Chase group exhibited superior recovery on tasks reflecting hand use (the spinal cord region targeted with Chase injections), and no difference in measures that included hindlimb function (i.e., those not targeted by Chase treatment). N=6 Chase subjects and N=5 Control subjects. Large data points show group means, small data points are individual subjects, error bars represent SEM.

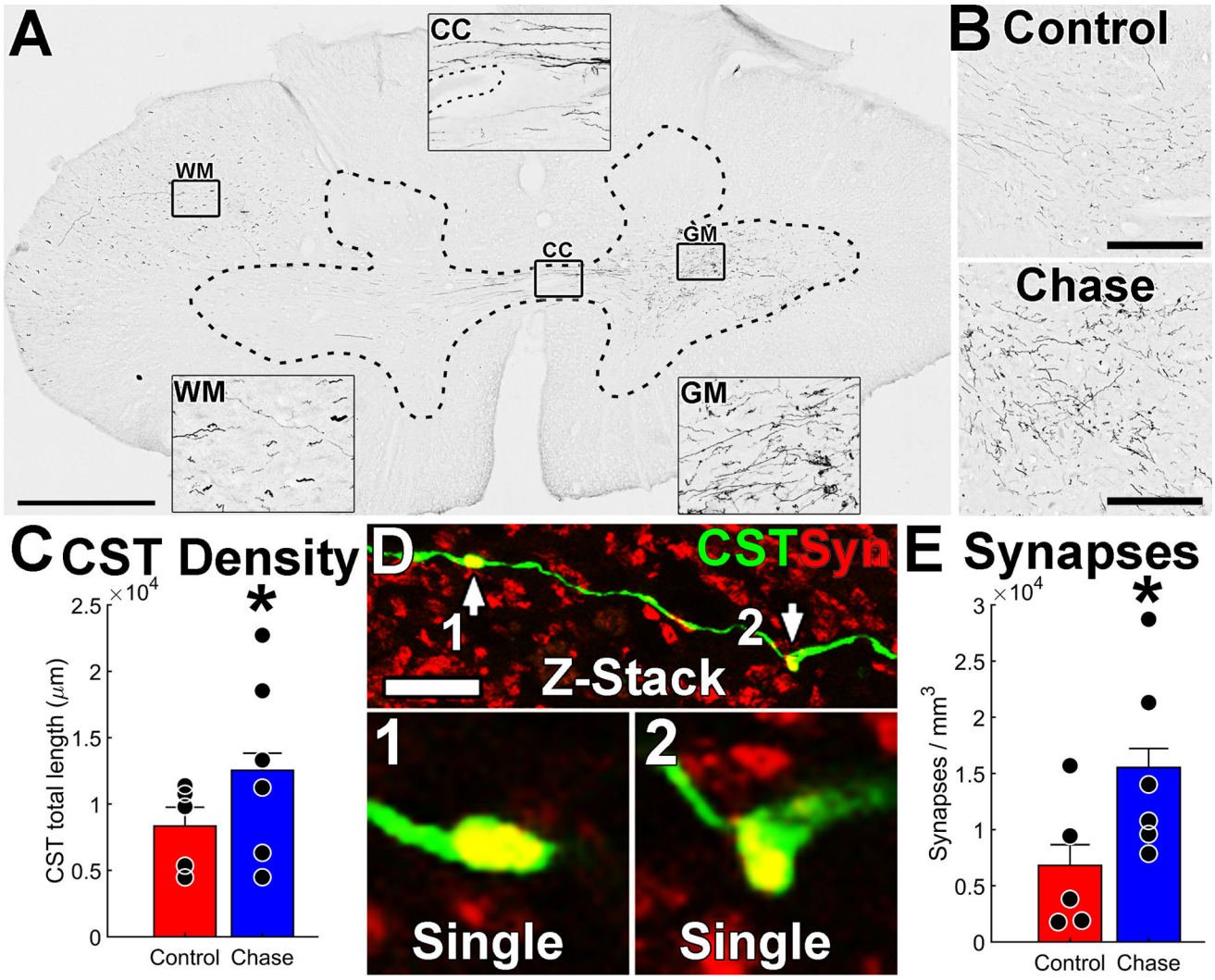

Figure 4: Effects of Chase on Corticospinal Axon and Synapse Density

(**A**) BDA-traced CST axons descending in the intact white matter (**WM**; left dorsolateral quadrant of spinal cord), crossing the spinal cord midline near the central canal (**CC, dashed line in inset**), and terminating in the gray matter (**GM**) on both sides of the spinal cord. **Dashed line** shows WM-GM boundary. Chase-treated subject, spinal level C8. (**B**) Representative images of gray matter from Chase-treated and control subjects at C8; note the qualitatively greater CST density in Chase-treated tissue. (**C**) Quantification of CST density in lesion-side gray matter indicates greater CST axon length per 40 μm tissue section in treated subjects (P=0.036, linear mixed model). (**D**) Two presumptive synapses in C8 gray matter. Top panel is a flattened z-stack of five 0.75 μm confocal optical sections, and shows two presynaptic boutons (**arrows**). Bottom panels are higher magnifications of single optical sections, demonstrating co-localization of synaptophysin in a bouton-like CST axon. (**E**) Quantification of synaptophysin bouton-like density identifies significantly more synapses per mm^3 in Chase-treated subjects (P=0.001, linear mixed model). N=6 Chase subjects and

N=5 Control subjects. Bar graphs show means, data points are individual subjects, error bars represent linear mixed model SEM. Scale bars: A, 1 mm; B, 100 μm; D, 10 μm.